Incoherence-Mediated Remote Synchronization

Liyue Zhang, Adilson E. Motter, and Takashi Nishikawa

Phys. Rev. Lett. **118**, 174102 — Published 28 April 2017

DOI: 10.1103/PhysRevLett.118.174102

Incoherence-Mediated Remote Synchronization

Liyue Zhang,[1,2] Adilson E. Motter,[2,3] and Takashi Nishikawa[2,3,*]

[1]*Center for Information Photonics and Communications, Southwest Jiaotong University, Chengdu, Sichuan 610031, China*
[2]*Department of Physics and Astronomy, Northwestern University, Evanston, IL 60208, USA*
[3]*Northwestern Institute on Complex Systems, Northwestern University, Evanston, IL 60208, USA*

In previously identified forms of remote synchronization between two nodes, the intermediate portion of the network connecting the two nodes is not synchronized with them but generally exhibits some coherent dynamics. Here we report on a network phenomenon we call *incoherence-mediated remote synchronization* (IMRS), in which two non-contiguous parts of the network are identically synchronized while the dynamics of the intermediate part is statistically and information-theoretically incoherent. We identify mirror symmetry in the network structure as a mechanism allowing for such behavior, and show that IMRS is robust against dynamical noise as well as against parameter changes. IMRS may underlie neuronal information processing and potentially lead to network solutions for encryption key distribution and secure communication.

Communication, broadly defined as information exchange between different parts of a system, is a fundamental process through which collective dynamics arises in complex systems. Network synchronization [1], whether it is complete synchrony [2] or a more general form of synchronization [3–7], is a primary example of such dynamics and is thought to be largely driven by node-to-node communication. However, it has recently been shown that so-called remote synchronization [8–15] is possible: two distant nodes (or groups of nodes) can synchronize even when the intermediate nodes are not synchronized with them. In this form of synchronization, the dynamics of different intermediate nodes generally show some level of coherence with each other, exhibiting, e.g., generalized synchronization or delay synchronization.

In contrast, in this Letter we consider a dynamical state of a network that we shall call *incoherence-mediated remote synchronization* (IMRS). The N nodes of the network are organized into three non-empty groups, A, B, and C, where A is connected with B, and B is connected with C, but A and C are not directly connected (as illustrated in Fig. 1). We assume that group B has at least two nodes, and that the nodes and links within each group form a connected subnetwork. IMRS is then characterized by (1) a node from group A (denoted node 1) and a node from C (denoted node N) that are identically synchronized (rather than in weaker forms such as phase and generalized synchronization), and (2) the dynamics of the nodes in the intermediate group B that are statistically incoherent with each other. IMRS combines the properties of remote synchronization mentioned above with those of chimera states [16–20], which are characterized by the coexistence of both coherent and incoherent dynamics in different parts of the network. Here, however, we lift the assumption of uniform network typically made in studying chimera states, and instead ask the following fundamental question: under what conditions can IMRS be observed? In particular, what types of network structure allow for this behavior? Below we answer these questions by mapping them to the problem of cluster synchronization and using a powerful tool for studying network symmetry based on computational group theory [7]. Moreover, we show that the incoherent dynamics of group B

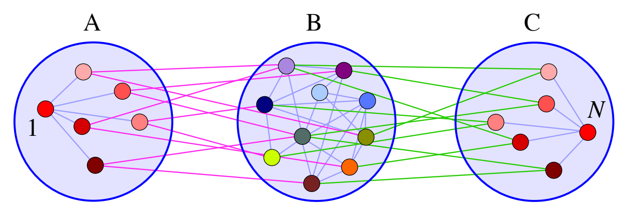

FIG. 1. Remote synchronization between node groups A and C mediated by incoherence in group B. The colors of the nodes schematically represent their states, indicating that nodes 1 and N are identically synchronized, while the dynamics of the nodes in B are incoherent.

is typically also incoherent relative to the dynamics of node 1 (and N). This suggests applications of IMRS to new forms of secure communication technologies [21, 22] or new schemes for secure generation and distribution of encryption keys [23].

We consider a general class of networks of N coupled identical dynamical units, whose time evolution is governed by

$$\dot{\mathbf{x}}_i = \mathbf{F}(\mathbf{x}_i) + \sigma \sum_{j=1}^{N} A_{ij} \mathbf{H}(\mathbf{x}_j), \tag{1}$$

where $\mathbf{x}_i(t)$ is the state of the ith unit at time t, $\dot{\mathbf{x}} = \mathbf{F}(\mathbf{x})$ describes the dynamics of an isolated node, σ is the overall coupling strength, $A = (A_{ij})_{1\le i,j\le N}$ is the coupling matrix representing an undirected unweighted network topology of the type illustrated in Fig. 1, and $\mathbf{H}(\mathbf{x})$ is a function determining the output signal from a node. Within this framework, we formulate a set of three conditions for IMRS to be observed:

(i) There exists a state in which $\mathbf{x}_1(t) = \mathbf{x}_N(t)$ for $\forall t$.

(ii) The state of synchronization between nodes 1 and N in condition (i) is stable.

(iii) $\{\mathbf{x}_i(t)\}$ and $\{\mathbf{x}_j(t)\}$ are not synchronized for all node pairs and are statistically incoherent for most pairs in B.

(Recall that nodes 1 and N are from groups A and C, respectively.)

Although condition (i) is dynamical in nature, a network-structural condition implying condition (i) can be expressed solely in term of the symmetry of the network. The network symmetry is represented by the (mathematical) group of node permutations under which the network structure is invariant (or, equivalently, of the corresponding permutation matrices that commute with the adjacency matrix A). A cluster of synchronized nodes can be identified as an orbit of this group, defined as a set of nodes in which each node can be mapped to any other by some permutation in the group. From the invariance of Eq. (1) under these permutations, it follows that there is a synchronous state in which all nodes in each orbit (of the group) have identical dynamics, forming K clusters: $\{\mathbf{s}_k(t)\}_{1\leq k\leq K}$, where $\mathbf{x}_i(t) = \mathbf{s}_k(t)$ for all t if node i belongs to cluster C_k. Note that $\mathbf{s}_k(t)$ can be different for different k as long as they satisfy the equations obtained by substituting $\mathbf{x}_i(t) = \mathbf{s}_k(t)$ into Eq. (1). Formulating IMRS as such a state, we see that condition (i) above is equivalent to the existence of an orbit that intersects with both A and C. We denote this cluster by C_1, from which we choose one node in A as node 1, and one node in C as node N.

The synchronization stability condition (ii) is verified for a given network structure using the method in Ref. [7]. We first identify clusters C_k in the network using computational group theory. We then compute λ_{C_1}, the maximum transverse Lyapunov exponent associated with the modes of perturbation that destroys the synchronization of cluster C_1 (and hence the synchronization between nodes 1 and N). Thus, condition (ii) can be formulated as $\lambda_{C_1} < 0$.

The statistical coherence in condition (iii) is measured by cross correlation and mutual information, accounting for possible coherence with a time lag Δt. We use $C_{i,j}$ to denote the absolute value of the Pearson correlation coefficient between $\mathbf{x}_i(t)$ and $\mathbf{x}_j(t+\Delta t)$ over a range of t, maximized over a range of Δt [24]. Likewise, we use $I_{i,j}$ to denote the mutual information between $\mathbf{x}_i(t)$ and $\mathbf{x}_j(t+\Delta t)$ over t, maximized over Δt [24, 25]. Thus, condition (iii) would be satisfied if $C_{i,j}$ and $I_{i,j}$ are both small for most pairs i and j in B, and $C_{i,j} \neq 1$ for $\forall i, j$ (indicating no identical synchronization). We choose chaotic node dynamics for higher likelihood of having incoherence in B, and we further ensure that the dynamics of $\mathbf{s}_k(t)$ is chaotic. This condition is equivalent to $\lambda > 0$, where λ is the maximum Lyapunov exponent parallel to the synchronization manifold (associated with perturbations that do not destroy synchronization of any cluster C_k).

Condition (iii) is also intimately related to network symmetry; it requires that each cluster in B contain only one node. What characterizes the structure of networks that satisfy both this requirement and condition (i)? Based on our numerical verification for $N \leq 8$ nodes, we conjecture that any such network has a mirror symmetry (possibly after regrouping the nodes): groups A and C are "mirror images" of each other (as illustrated in Fig. 1). More precisely, the network structure is invariant under a node permutation that serves the role of a "reflection" and maps each node in A to a unique node in C, but does not move any nodes in B. In particular, this implies that each node in B that connects to A must connect to C in exactly the same way. It also implies that all nontrivial clusters (i.e., those of size > 1), which we denote $C_1, \ldots, C_{K'}$ (after appropriate re-indexing), span both A and C in a symmetrical way (involving the same number of nodes from each group) and collectively cover all nodes in A and C. This means that the corresponding network dynamics is also mirror-symmetric: each node in A is identically synchronized with its counterpart in C (possibly showing different dynamics for different node pairs). In particular, we have identical synchronization between nodes 1 and N (both belonging to C_1). Moreover, the clusters $C_1, \ldots, C_{K'}$ are all intertwined with each other, i.e., synchronization of these clusters must be either all stable or all unstable. A group-theoretical origin of this behavior is argued to be the property that any network-invariant permutation that swap the nodes in one cluster must also swap the nodes in each of the other clusters [7], which we conjecture is guaranteed by the mirror symmetry. Conversely, if a network with the three-group structure of Fig. 1 has a mirror symmetry, then nodes 1 and N (in A and C, respectively) are guaranteed to be part of a synchronized cluster. Note that the mirror symmetry alone does not impose any condition on the link configuration within B, and hence the clusters in B can in principle be of size > 1 [which would violate condition (iii)].

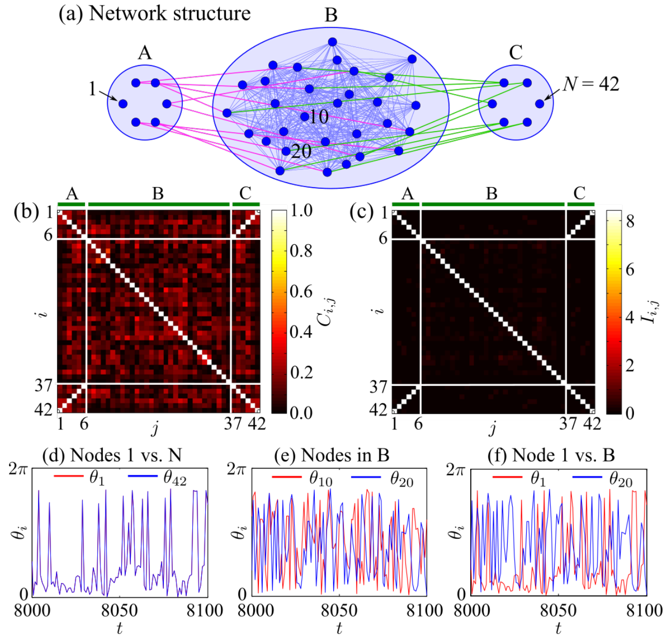

FIG. 2. Network exhibiting IMRS. (a) Mirror-symmetric structure of the network, generated with $n_\mathrm{A} = 6$, $n_\mathrm{B} = 30$, $n'_\mathrm{B} = 2$, and $p = 0.8$. (b) Pairwise cross correlation $C_{i,j}$. (c) Pairwise mutual information $I_{i,j}$. (d)–(f) Phase variable θ_i as a function of t. In (d), only the blue curve is clearly visible because the two curves overlap. The calculations in (b)–(f) are based on iterating Eq. (2) with $\beta = 1.5$ and $\sigma = 1.5$.

To systematically search for IMRS, we propose the following general recipe for designing a system: 1) construct an arbitrary network structure that has a mirror symmetry and satisfies the size-one cluster requirement in B; 2) select chaotic node dynamics; 3) find system parameters for which the synchronization between nodes 1 and N is stable (i.e., $\lambda_{C_1} < 0$) and the dynamics of $\mathbf{s}_k(t)$ is chaotic (i.e., $\lambda > 0$); and 4) verify incoherence in B (i.e., small $C_{i,j}$ and $I_{i,j}$). As an example algorithm for generating networks for step 1 above, we use the following procedure (for which we provide software; see SM [26]). Given n_{A}, n_{B}, and n_{C} $(= n_{\mathrm{A}})$ nodes in A, B, and C, respectively, we first connect each pair of nodes in B with probability p. Next, we connect node 1 to all the other nodes in A and node N to all the other nodes in C. The nodes in A other than node 1 are then paired up with the nodes in C other than node N. Finally, for each of these node pairs, we choose n'_{B} nodes randomly from B and connect each of these nodes to the node pair. An example network constructed by this procedure is shown in Fig. 2(a). The probability of having a cluster of size > 1 in B can be kept small by making the size of B large enough. Here we generate networks with $n_{\mathrm{B}} \geq 10$ and use only those with no cluster of size > 1 in B.

As an example dynamics for the network leading to IMRS, we use coupled maps that model the electro-optic experimental system [18], although we anticipate that continuous-time systems will also exhibit IMRS (see SM [26], Sec. S1). The system dynamics is governed by

$$\theta_i^{t+1} = \left[\beta I\left(\theta_i^t\right) + \sigma \sum_{j=1}^{N} A_{ij} I\left(\theta_j^t\right) + \delta\right] \bmod 2\pi, \tag{2}$$

where θ_i^t is the phase shift in time step t for the ith component of the spatial light modulator array used in the experiment, β is the strength of self-feedback coupling for the array components, and the offset δ is introduced to suppress the trivial solution, $\theta_i^t \equiv 0$. We set $\delta = 0.525$ for all computations for this system. The intensity of light is related to spatially dependent phase shift θ through the nonlinear function $I(\theta) := [1-\cos(\theta)]/2$. The dynamics of an isolated oscillator has a globally stable fixed point for small β, which, through a sequence of period-doubling bifurcations, becomes chaotic for larger values of β [see Fig. 3(a)].

As shown in Fig. 3(b), we find that networks generated by the procedure described above can achieve $\lambda_{C_1} < 0$ (i.e., stable synchronization between nodes 1 and N) when β and σ are both relatively small. Since these networks all have a mirror symmetry by construction, they satisfy both conditions (i) and (ii). Figure 3(c) shows that, even when we start with oscillators that are not chaotic in isolation [$\beta \lesssim 4$, see Fig. 3(a)], the dynamics of the clusters $\mathbf{s}_k(t)$ becomes chaotic (i.e., $\lambda > 0$) as the coupling strength σ is increased. We thus see that there is a wide range of parameters β and σ for which the network realizes stable chaotic synchronization. To check condition (iii), we compute $C_{i,j}$ and $I_{i,j}$ over time steps $10^4 \leq t \leq 4 \times 10^4$ and time delay $-50 \leq \Delta t \leq 50$ for $\beta = 1.5$ and $\sigma = 1.5$ [black crosses in Figs. 3(b) and 3(c)]. The results, shown in Figs. 2(b) and 2(c), verify that condition (iii) is indeed satisfied. The corresponding system dynamics is illustrated by the time plots in Figs. 2(d)–(f). Thus, the network exhibits IMRS for these specific parameters. Moreover, Figs. 2(b) and 2(c) clearly show that the dynamics of the nodes in B is also incoherent relative to nodes 1 and N. While Eq. (2) is a discrete-time analog of Eq. (1), we expect IMRS to be observed for a range of different node dynamics, including both discrete-time and continuous-time dynamics, as well as for many mirror-symmetric network topologies not necessarily generated by the procedure described above.

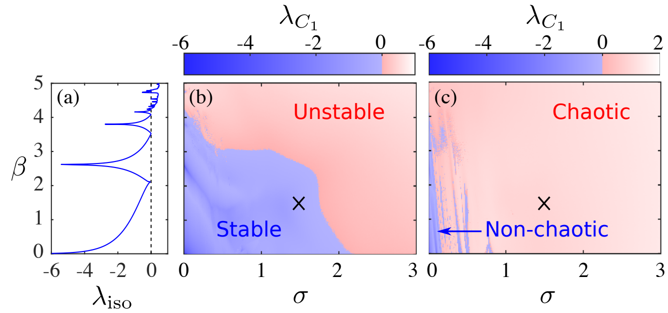

FIG. 3. Characterizing the network dynamics. (a) Lyapunov exponent λ_{iso} of the isolated node dynamics as a function of self-feedback strength β. (b) Synchronization stability λ_{C_1} of cluster C_1 (and thus between nodes 1 and N) as a function of β and coupling strength σ. (c) Lyapunov exponent λ measuring the instability parallel to the synchronization manifold as a function of β and σ. The exponents λ_{C_1} and λ are averaged over 10 network realizations and 10 initial conditions.

How does IMRS depend on system parameters? To answer this question, we study the distribution of $C_{i,j}$ (Fig. 4) and $I_{i,j}$ (Fig. S2 in Sec. S2 of SM [26]) over all $i \neq j \in \mathrm{B}$ as functions of parameters n_{B}, n'_{B}, n_{A}, β, and σ. We verify $\lambda_{C_1} < 0$ for the entire range of parameter values over which the curves are drawn in Fig. 4 (see SM [26], Sec. S2 for more details, including parameter dependence of λ_{C_1}). As indicated by their 75th and 25th percentiles (dashed curves), the cross correlation and mutual information remain low for most node pairs in B for a range of system parameters, with the exception of cases with small σ. The medians of these coherence measures are mostly monotonically decreasing functions of σ up to the maximum value of σ $(= 1.7)$ for which $\lambda_{C_1} < 0$ [Fig. 4(e) and Fig. S2(e)]. We have $C_{i,j} = 1$ at $\sigma = 0$, indicating that all nodes in B are perfectly correlated in that case, simply because the isolated oscillators all converge to a common stable fixed point for $\beta = 1.5$. The median cross correlation and the median mutual information appear to be slightly decreasing functions of n_{B} and n'_{B}, while they seem to be approximately constant as functions of n_{A} (both for $\sigma = 1.5$ and $\sigma = 1$) and β. Note, however, that the synchronization stability does depend on n_{A}: we observe that nodes 1 and N cannot synchronize stably for $n_{\mathrm{A}} > 6$ for $\sigma = 1.5$ [green curves ending at $n_{\mathrm{A}} = 6$ in Fig. 4(c) and Fig. S2(c)] but remain stably synchronized up to $n_{\mathrm{A}} = 15$ for $\sigma = 1$ [blue curves in Fig. 4(c) and Fig. S2(c)]. The loss of synchronization stability for sufficiently large n_A is likely due to incoherent dynamics of the other nodes in groups A and C (see SM [26], Sec. S3). Since these nodes are the only ones that directly influence the dy-

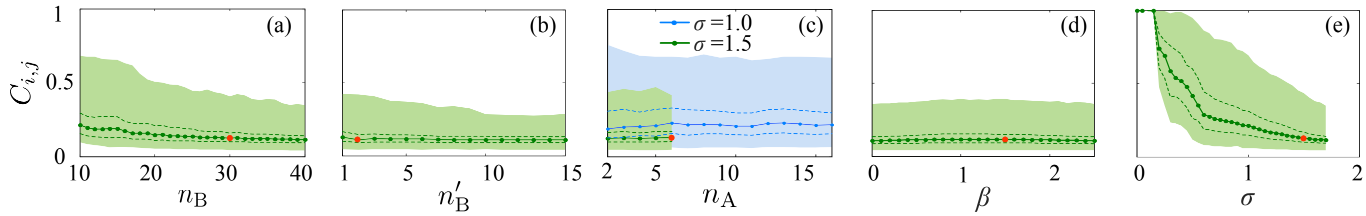

FIG. 4. Influence of system parameters on IMRS. The distribution of the correlation $C_{i,j}$ between pairs of nodes in B is shown as a function of parameters n_B, n'_B, n_A, β, and σ. Each panel shows the median (solid curve with dots), the minimum and maximum defining the range (shaded region), as well as the 75th and 25th percentiles (dashed curves). These quantities are all averaged over 10 network realizations and 10 initial conditions. Unless noted otherwise, all parameters are set to the values used in Fig. 2 (indicated by red dots).

namics of nodes 1 and N (and thus their synchronization stability), the larger the number of these dynamically incoherent nodes (i.e., the larger n_A), the more difficult for nodes 1 and N to stably synchronize. Overall, we find that IMRS is observed for a wide range of structural and dynamical parameters of the system (see SM [26], Sec. S4 for similar robustness observed for a continuos-time system).

We also find that the low levels of coherence between node 1 (or N) and the nodes in B is maintained over a range of parameter values, following dependence patterns similar to those of the coherence levels within B (see SM [26], Sec. S5). Low coherence between periphery and intermediate nodes has also been observed in certain cases of remote synchronization [10, 11] [but with pairs of identically synchronized oscillators in the intermediate part of the network, which violates the IMRS condition (iii)].

An key aspect of IMRS lies in its behavior against noise. While the synchronization of nodes 1 and N is robust against independent noise added to the dynamics in A and C only up to a certain level (which is expected), IMRS is completely insensitive to noise in B, even when the noise level is very high (see SM [26], Sec. S6). This characteristic robustness of IMRS stems from the mirror symmetry and is also associated with the dynamical incoherence in condition (iii). In contrast, (remote) synchronization of nodes 1 and N can be extremely sensitive to noise in B when some nodes in B are identically synchronized. This is demonstrated using the network topology considered in Ref. [10] (see SM [26], Sec. S7).

Our demonstration of IMRS challenges the notion that paths of communication between nodes that are exchanging information should be somehow observable. A particularly striking feature of IMRS we studied here is that the coupling between A and B, as well as B and C, is bidirectional. This allows information to be transferred from A to C through B, despite the scrambling of that information by the incoherent chaotic dynamics of B, which reduces the amount of shared information in B to a level that is too low for eavesdroppers (as measured by mutual information). This feature fundamentally sets IMRS apart from a master-slave type of chaos synchronization [27], in which the dynamics of B influences that of A and C, but not vice versa, thus prohibiting communication between nodes 1 and N. The same behavior can be observed even when B is replaced by noise, if the average of the noise is nonzero and its effect is equivalent to parameter change that drives the dynamics into synchrony [28].

A defining characteristic of IMRS we demonstrated here is the dynamical incoherence within group B, which is enabled by the mirror symmetry we established as a general condition for observing IMRS. While we focused on undirected networks here, an analog of mirror symmetry can be formulated for directed networks using the notion of input equivalence [4]. Since zero-lag synchronization of distant areas of the brain has been experimentally observed [29–31], our results suggest the intriguing possibility that a mirror symmetry is hidden deep inside the synaptic connectivity structure. We hope that our discovery will spark interests of many researchers and lead to further discoveries of fundamental connections between hidden network symmetry and emergent collective behavior in complex systems.

This work was supported by the NSFC (Award No. 61274042), CSC, 2013 Doctoral Innovation Funds of SWJTU, and ARO (Award No. W911NF-15-1-0272). The authors thank Prof. Wei Pan for comments on the manuscript.

* t-nishikawa@northwestern.edu

[1] A. Pikovsky, M. Rosenblum, and J. Kurths, *Synchronization: A Universal Concept in Nonlinear Sciences* (Cambridge University Press, Cambridge, England, 2003).
[2] L. M. Pecora and T. L. Carroll, Master stability functions for synchronized coupled systems, Phys. Rev. Lett. **80**, 2109 (1998).
[3] K. Kaneko, Clustering, coding, switching, hierarchical ordering, and control in a network of chaotic elements, Physica D **41**, 137 (1990).
[4] I. Stewart, M. Golubitsky, and M. Pivato, Symmetry groupoids and patterns of synchrony in coupled cell networks, SIAM. J. Appl. Dyn. Syst. **2**, 609 (2003).
[5] F. Sorrentino and E. Ott, Network synchronization of groups, Phys. Rev. E **76**, 056114 (2007).
[6] T. Dahms, J. Lehnert, and E. Schöll, Cluster and group synchronization in delay-coupled networks, Phys. Rev. E **86**, 016202 (2012).
[7] L. M. Pecora, F. Sorrentino, A. M. Hagerstrom, T. E. Murphy, and R. Roy, Cluster synchronization and isolated desynchronization in complex networks with symmetries, Nat. Commun. **5**, 4079 (2014).
[8] H. G. Winful and L. Rahman, Synchronized chaos and spatiotemporal chaos in arrays of coupled lasers, Phys. Rev. Lett.

65, 1575 (1990).

[9] I. Fischer, R. Vicente, J. M. Buldú, M. Peil, C. R. Mirasso, M. C. Torrent, and J. García-Ojalvo, Zero-lag long-range synchronization via dynamical relaying, Phys. Rev. Lett. **97**, 123902 (2006).

[10] G. Van der Sande, M. C. Soriano, I. Fischer, and C. R. Mirasso, Dynamics, correlation scaling, and synchronization behavior in rings of delay-coupled oscillators, Phys. Rev. E **77**, 055202 (2008).

[11] M. C. Soriano, G. Van der Sande, I. Fischer, and C. R. Mirasso, Synchronization in simple network motifs with negligible correlation and mutual information measures, Phys. Rev. Lett. **108**, 134101 (2012).

[12] A. Bergner, M. Frasca, G. Sciuto, A. Buscarino, E. J. Ngamga, L. Fortuna, and J. Kurths, Remote synchronization in star networks, Phys. Rev. E **85**, 026208 (2012).

[13] A. Viriyopase, I. Bojak, M. Zeitler, and S. Gielen, When long-range zero-lag synchronization is feasible in cortical networks, Front. Comput. Neurosci. **6**, 49 (2012).

[14] V. Nicosia, M. Valencia, M. Chavez, A. Díaz-Guilera, and V. Latora, Remote synchronization reveals network symmetries and functional modules, Phys. Rev. Lett. **110**, 174102 (2013).

[15] L. V. Gambuzza, A. Cardillo, A. Fiasconaro, L. Fortuna, J. Gómez-Gardeñes, and M. Frasca, Analysis of remote synchronization in complex networks, Chaos **23**, 043103 (2013).

[16] Y. Kuramoto and D. Battogtokh, Coexistence of coherence and incoherence in nonlocally coupled phase oscillators, Nonlinear Phenom. Complex Syst. **5**, 380 (2002).

[17] D. M. Abrams and S. H. Strogatz, Chimera states for coupled oscillators, Phys. Rev. Lett. **93**, 174102 (2004).

[18] A. M. Hagerstrom, T. E. Murphy, R. Roy, P. Hövel, I. Omelchenko, and E. Schöll, Experimental observation of chimeras in coupled-map lattices, Nat. Phys. **8**, 658 (2012).

[19] M. R. Tinsley, S. Nkomo, and K. Showalter, Chimera and phase-cluster states in populations of coupled chemical oscillators, Nat. Phys. **8**, 662 (2012).

[20] M. J. Panaggio and D. M. Abrams, Chimera states: coexistence of coherence and incoherence in networks of coupled oscillators, Nonlinearity **28**, R67 (2015).

[21] K. M. Cuomo, A. V. Oppenheim, and S. H. Strogatz, Synchronization of Lorenz-based chaotic circuits with applications to communications, IEEE Trans. Circuits Syst. II **40**, 626 (1993).

[22] A. Argyris *et al.*, Chaos-based communications at high bit rates using commercial fibre-optic links, Nature **438**, 343 (2005).

[23] H. Koizumi *et al.*, Information-theoretic secure key distribution based on common random-signal induced synchronization in unidirectionally-coupled cascades of semiconductor lasers, Opt. Exp. **21**, 17869 (2013).

[24] L. Zhang *et al.*, Conceal time-delay signature of mutually coupled vertical-cavity surface-emitting lasers by variable polarization optical injection, IEEE Photon. Technol. Lett. **24**, 1693 (2012).

[25] T. M. Cover and J. A. Thomas, *Elements of Information Theory* (John Wiley & Sons, 1991).

[26] See Supplemental Material for results on networks of coupled Lorenz oscillators and other supporting details. Supplemental Material also includes MATLAB code (`mirror_sym_net.m`) for generating the random mirror-symmetric networks used in our study.

[27] L. M. Pecora and T. L. Carroll, Synchronization in chaotic systems, Phys. Rev. Lett. **64**, 821 (1990).

[28] H. Herzel and J. Freund, Chaos, noise, and synchronization reconsidered, Phys. Rev. E **52**, 3238 (1995).

[29] P. R. Roelfsema, A. K. Engel, P. König, and W. Singer, Visuomotor integration is associated with zero time lag synchronization among cortical areas, Nature **385**, 157 (1997).

[30] E. Rodriguez *et al.*, Perception's shadow: long-distance synchronization of human brain activity, Nature **397**, 430 (1999).

[31] D. S. Soteropoulus and S. N. Baker, Cortico-cerebellar coherence during a precision grip task in the monkey, J. Neurophysiol. **95**, 1194 (2006).